

# HEAVY ION FUSION EXPERIMENTS AT LBNL AND LLNL\*

Larry Ahle (presented for the groups at LBNL and LLNL)  
Lawrence Livermore National Laboratory, Livermore, CA 94551 USA

## Abstract

The long-range goal of the US Heavy Ion Fusion (HIF) program is to develop heavy ion accelerators capable of igniting inertial fusion targets to generate fusion energy for electrical power production. Accelerators for heavy ion fusion consist of several subsystems: ion sources, injectors, matching sections, combiners, induction acceleration sections with electric and magnetic focusing, beam compression and bending sections, and a final-focus system to focus the beams onto the target. We are currently assembling or performing experiments to address the physics of all these subsystems. This paper will discuss some of these experiments.

## 1 HEAVY ION FUSION DRIVER

In a heavy ion inertial power plant, particle beams are focused onto a target causing ignition. These targets consist of a hohlraum with a Beryllium (or other low  $Z$  ablator material) capsule inside. The capsule surrounds a frozen spherical shell of D-T, which is heated and compressed by X-rays created from the stopping of the ions in the hohlraum. The accelerator will need to provide approximately 5-MJ of energy on a time scale of  $\sim 10$ -ns for ignition [1] and at a rate of  $\sim 5$ -Hz for a cost effective power plant [2]. Further, the range of the ion beams should be roughly  $0.1$ -g/cm<sup>2</sup> which implies a total kinetic energy per beam particle of a few GeV.

The target specifications above are now based on sophisticated simulation validation and are generally demanding lower emittance beams than believed necessary a few years ago. There also appears to be a trade off between beam current and ion kinetic energy. Higher beam current implies a higher technical risk but the resulting lower energy may produce a cheaper power plant.

Current conceptual designs for a heavy ion fusion driver start with  $\sim 100$  beam 2-MeV injector and ESQ matching section providing a initial pulse of 20- $\mu$ s with approximately 1-A of current for each beam with radius of several centimeters. This is followed by an accelerator section. Whether the initial part of the accelerator is electrostatically focused, followed by beam merging, or magnetically focused is still being studied, but the end of the accelerator will be magnetic. The acceleration is accomplished through magnetic induction cores at the rate

of 1-MV/m through most of the machine. The pulses on these induction cores are tilted to longitudinally compress the pulse from an initial length of  $\sim 30$ -m to  $\sim 10$ -m, which corresponds to a pulser duration of about 100-ns at the end of the accelerator. Following this is the drift compression, final focus, and target chamber section. The drift compression will do the final longitudinal compression to  $\sim 1$ -m in length. The final focus section will focus the beam to the target in the chamber reducing the radius of the beam to a few millimeters.

## 2 SOURCE AND INJECTOR

In developing sources and injectors for a driver, high current density is desired because it allows smaller and/or fewer beams and thus a cheaper injector. The current density is limited by voltage breakdown in the injector and transport limitations in the accelerator section and not by the emission limit of the source itself. Currently the design goal of an injector for a driver is many beam channels in one single vacuum chamber with a current density of 8-mA/cm<sup>2</sup> Cs equivalent.

### 2.1 Source Development

There are many possible types of ion sources for HIF, generally producing singly charged ions but higher charge states are also of interest in some driver designs. Surface ionization sources provide alkali metal ions, while a gas source is suitable for generating Hg, Xe, Ar and Ne ions, and a metal vapor vacuum arc source (MEVVA) would be more appropriate for ions such as Gd and Bi. Most HIF induction linac designs have used surface ionization sources because their performance already approaches the HIF requirements.

LBNL has been working with two types of surface ionization sources, contact ionizer and aluminosilicate. In a contact ionizer, alkali atoms are continuously fed to a heated surface, which ionizes the atoms. This type of source routinely produces low emittance and highly uniform beams. It also has the potential for a long lifetime source, but since alkali metal vapor deposits can deteriorate the high voltage property of accelerator components, it is important to minimize the cesium flow. In a recent experiment [3], the Cs<sup>+</sup> beam current from a 2-cm diameter contact ionizer was measured to be  $> 15$ -mA/cm<sup>2</sup> at 1145°C. In addition, the rate of the cesium neutral current evaporation was measured to be  $1.7 \times 10^{14}$ /cm<sup>2</sup>/s or equivalently 0.14 mg/cm<sup>2</sup>/hr. To test these sources in a real application, a Cs<sup>+</sup> contact ionizer will be installed in the scaled final focus experiment

\* Work supported by the US DOE under contract No. DE-AC03-76SF00098 (LBNL) and W-7405-ENG-48 (LLNL).

described in section 4.2. This source will provide a factor of four increase in the current density and a more uniform beam.

For aluminosilicate sources, a layer of aluminosilicate doped with an alkali metal, is melted on a tungsten surface. This tungsten surface is then heated during operation. The neutral current for these sources should be lower than for the contact ionizer [4], but its lifetime for a driver before ion depletion is about one month [5]. Current densities of  $\approx 15\text{-mA/cm}^2$  of potassium,  $7.9\text{-mA/cm}^2$  Cs equivalent, have been achieved with a 2-cm aluminosilicate source [3]. For these sources to achieve uniform emission and high current density, a smooth layer must be melted on a large spherical area, which has proven to be a significant technical challenge. Recently, a different method to produce the aluminosilicate sources, in which a mixture of aluminosilicate and tungsten powder is sintered to form an emitter has been adopted [6].

## 2.2 2 MeV Injector

Based on ESQ beam transport considerations, a 2-MeV driver-scale injector should provide beams with a line charge density of approximately  $0.25 \times 10^{-6}$  C/m. A prototype injector, as shown in figure 1, was built for the Elise/ILSE project. It consists of a 17-cm diameter potassium aluminosilicate source as part of a 750-kV extraction diode which is in series with a 1250 kV ESQ accelerator. Both diode and ESQ are powered by a Marx Generator using a resistive divider. The column is completely enclosed in a steel tank (at 80 PSI compressed gas atmosphere) for compatibility with using SF<sub>6</sub>.

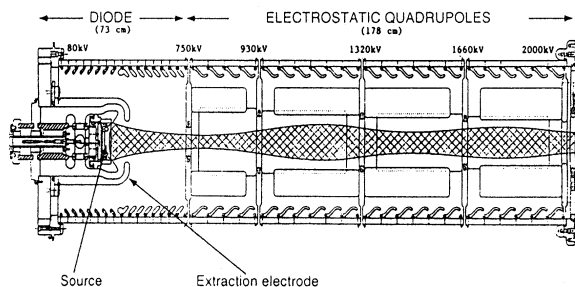


Figure 1: Schematic diagram of the 2-MeV injector.

Earlier tests have demonstrated beam current of up to 0.8 A of potassium ions (space-charge-limited) with a  $\epsilon_{4\text{rms}}$  projectional emittance  $< 1.0 \pi\text{-mm-mrad}$  [7]. However, it was also discovered that the beam current density profile at the end of the injector has a hollow shape instead of the calculated uniform shape. In order to find out what causes the beam non-uniformity, a movable Faraday cup array was recently constructed to measure the beam profile at locations (along beam axis) inside the ESQ accelerator. Some preliminary data indicates the problem may occur at the extraction diode. At present, a new contact ionizer source of the same dimension is being prepared to replace the aluminosilicate source in order to

determine if the phenomenon is related to non-uniform ion emission.

## 3 THE ACCELERATOR

### 3.1 Beam Merging

Transverse beam combining at the transition from electrostatic to magnetic quadrupole transport could lower the cost of a multiple beam induction linac driver. The cost of induction core material and HV breakdown dictate a small aperture in electrostatic quadrupoles, while magnetic quadrupole transport -- very effective at higher kinetic energy, favors larger apertures (and fewer beams). The challenge for beam merging is to limit resulting emittance growth (minimized by closely packing the merged beams in phase space [8]).

The 4-to-1 beam combining experiment [9] is designed to establish the ability to merge beams with considerable space charge, and measure the phase space evolution of the merged beams. The four initial Cs<sup>+</sup> beams are generated in 160 kV diodes and initially converge at a 6° angle relative to the combiner center line. Four arrays of electrostatic quadrupoles (Q1-Q4) followed by the combined function dipole-quadrupole element (“wire cage”, QD5) focus each beam and straighten its trajectory to be parallel to the downstream transport line. After the wire cage, the merged beam is transported and diagnosed at several locations along the merged beam transport line (Q6-Q67).

We reported earlier [10] measuring 88% transmission through the combiner. These data indicated that the beam edge to beam edge separation was  $< 4$  mm at the merge point, with the 1 mm tungsten rods (of the wire cage) in between. The measured phase space between Q7 and Q8 (one lattice period downstream of the cage) was in agreement with the 2D PIC simulations. The initial beams (4.5-mA) had a factor 1.65 more current than originally thought compatible with the transport of merged beams in the (previously existing) downstream transport lattice. As a consequence of the higher current there was not enough clearance between the merged beam and electrodes in the matching quadrupoles (Q6-Q11) to enable further transport without significant beam loss.

Recently, each initial beam current has been lowered to 2.7-mA by altering the Pierce electrodes. This has improved beam matching through the combined function element and the 10.4-mA merged beam through the first downstream lattice period has several millimeters more clearance to the quadrupole electrodes. Beam loss in the transport lattice following the merge should also be negligible, allowing a more quantitative interpretation of the merged beam distribution function.

Figure 2 shows the phase space measured in the vertical plane between Q7 and Q8. Though the beam distribution function has not equilibrated at this point, the rms emittance,  $\epsilon_n \approx 0.2 \pi\text{-mm-mR}$ , has decreased by a factor

$\sim 0.5$  compared to the previous measurements with the higher beam current reported in [10]. Transport measurements through Q67 are currently underway. These results will establish some limits on emittance growth through for this approach to beam merging.

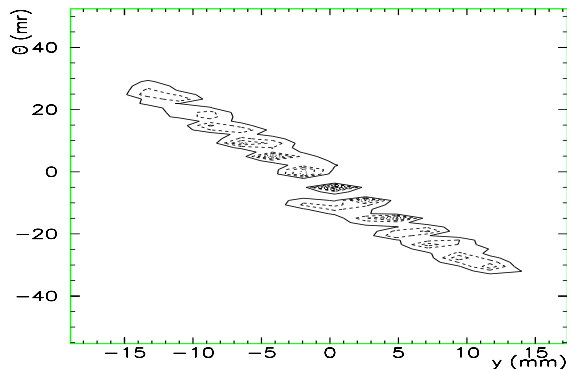


Figure 2: Contour plots from two-slit emittance scan of the merged beams between Q7 and Q8.

### 3.2 The Recirculator

Most designs of a driver are linear machines, but using a circular machine may provide significant cost savings. Such a machine, a circular ion induction accelerator for space charge dominated beams, or recirculator, have never been built before. Thus, a group at LLNL has been developing a small recirculator in order to validate the recirculator concept for an IFE power plant driver.

In designing this machine, all of the important dimensionless beam parameters, such as perveance, were kept the same as a full scale driver machine. Each half lattice period (HLP) of the recirculator consists of a permanent magnetic quadrupole for focusing, an electrostatic dipole for bending the beam, and an induction core, or modulator, for acceleration and longitudinal compression. The dipole plates are designed to provide a 9 degree bend to the beam while the modulators are designed to provide 500-eV of acceleration.

In the fall of 1997, the machine was extended from a 45 degree bend to a 90 degree bend section. Figure 3 shows the current layout of the machine. Initially, a 4- $\mu$ s beam pulse is injected by a source diode with an energy of 80-keV through an aperture of diameter 1-cm which provides an initial beam current of 2-mA. Upon injection the beam enters an electrostatic matching section which is followed by a short magnetic transport section before the 90 degree bend section. Following the bend section is the End Tank which houses several diagnostics. As part of the upgrade, magnetic induction cores were added to 5 of the 10 HLP's as shown.

The first attempts at beam transport through the 90 degree section were done with no acceleration and DC voltages ( $\pm 6.575$ -kV) on the bending dipole plates. Full current transport was achieved with less than 1% loss as measured by Faraday Cups. The RMS normalized

emittance for the 90% of full beam current was also measured at the source injector,  $0.021 \pi$ -mm-mR, and after 90 degrees,  $0.045\pi$ -mm-mR in x and  $0.068 \pi$ -mm-mR in y. The growth seen is within the design specifications.

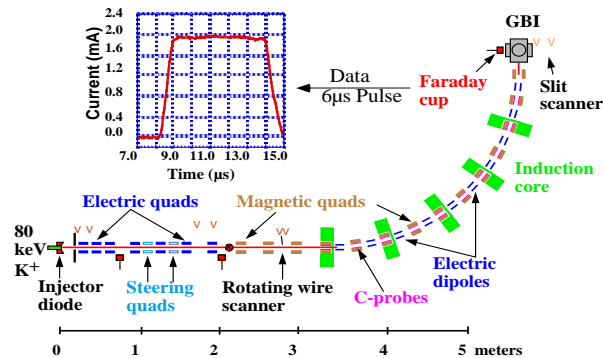


Figure 3: Current Recirculator Layout.

A network of C-probes (capacitively coupled beam position monitors) before and throughout the bend section has been enabled to measure the transverse beam position as a function of time. All four signals from each C-probe are amplified, digitized, and analyzed through the computer control system to obtain the charge centroid. Bench tests of the system using a conducting rod to simulate the beam have yielded a resolution of 70  $\mu$ m. Figure 4 shows the x position measured by the C-probes for various dipole voltages.

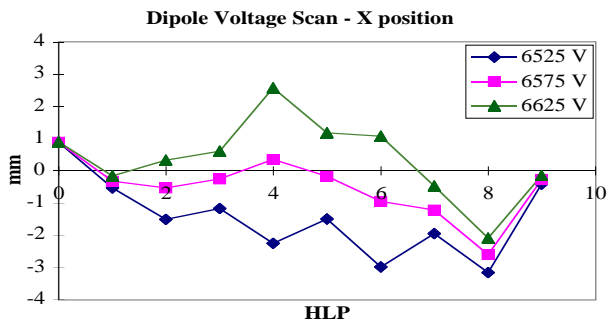


Figure 4: Time averaged X positions as measured by C-probes for various dipole voltages.

LLNL has developed a new device to measure the emittance, the Gated Beam Imager (GBI). The GBI is based on the pepperpot design in which the beam is incident on a hole with 100  $\mu$ m diameter holes creating many beamlets. Each beamlet is allowed to drift to a micro channel plate(MCP) which is coated with a thin layer of stainless steel,  $\sim 150$  nm, to stop the ions and produce secondary electrons. After passing through the MCP, the electrons are proximity focused on to a phosphor screen, and the light generated is focused and captured on a CCD camera. Recently, after the analysis of the GBI images was changed to more closely mimic the more traditional slit scan, the GBI was fully reconciled with the slit scanner.

Currently the initial implementation of the electronics necessary for acceleration and ramped dipole voltages, is underway. The first attempts at acceleration should occur shortly. For more information about the recirculator, please refer to the paper in these proceedings [11].

### 3.3 Induction Core Material

Currently one of the major cost items for a driver is the price of magnetic material for the induction cores. Recently, a survey of various commercially available material was done [12]. Two type of materials were tested, amorphous alloys and nanocrystalline alloys. The amorphous alloys cost less, have slightly higher flux swing (about a factor of 1.2), but have a significantly higher energy loss (about a factor of 5) than the nanocrystalline material. The important figure of merit for selection of material is the final cost of electricity. Obviously the nanocrystalline material will mean a lower operating cost, but a higher capital cost. System studies to determine which of these two materials produces a lower cost of electricity are underway.

## 4 FINAL FOCUS

There are several proposed schemes, depending on the intensities of the beams, for achieving the final spot size necessary to hit the target. At low intensities, vacuum ballistic focusing would suffice, but at high intensities a scheme involving charge neutralization or establishing a focusing current in a plasma must be invoked. Currently experiments are being performed investigating the ballistic focus scheme and one of the more exotic schemes, plasma channel transport [13].

### 4.1 Plasma Channel Transport

Plasma channel experiments, for heavy ion transport, are being conducted at LBNL to measure their time and space resolved plasma density evolution. These channel experiments are scaled versions that provide understanding of the channel's behavior under different regimes or parameter space, such as pressure, gas type, and discharge energy deposition, which directly relate to the transport efficiency. A working reactor ion transport design relies on proper selection of these parameters.

The plasma channel in these experiment are produced by a double voltage discharge technique initiated by the creation of a preferential discharge path produced by a KrF excimer laser. Plasma density space profiles have been obtained at several times during the first quarter cycle of channel current (peak current 29 kA). The measured pinch occurring (7 Torr N<sub>2</sub>, 200 mTorr Benzene, 15 kV discharge) at  $t=2.2$  microseconds is in agreement with previous experiments.

These measurements were made using a Michelson-type optical interferometer (1064 nm) with a time resolution of approximately 20 ns, determined by the probe laser pulse width. The on-axis plasma density time evolution ( $n_e =$

$1.3 \times 10^{17} \text{ cm}^{-3}$  at pinch time) provides input to the determination of a plasma conductivity model to be implemented in computer simulations.

Future experiments include the use of spectroscopy of the plasma's emitted radiation to measure the Zeeman and Stark broadening, as well as the Faraday rotation technique. These experiments will permit the mapping of the channel's magnetic field distribution and time evolution as well as the determination of its electron temperature.

### 4.2 Scaled Focusing Experiment

Vacuum ballistic focusing is one method to achieve the heavy ion beam spot size necessary for an inertial confinement fusion target. Proper scaling of particle energy, mass, beam current, beam emittance, and magnetic field replicates the dynamics of a full driver beam in a small laboratory beam. Thus, a one-tenth scale experiment, based on the HIBALL II design, is currently being assembled at LBNL. This scaled experiment uses a K<sup>+</sup> ion source to send a 120 keV beam through an aperture and electrostatic matching section. Approximately 80  $\mu\text{A}$  of beam is then sent through a set of six magnetic quadrupoles that comprise the final focus. By expanding the beam and then focusing to a very small spot, the effects of aberrations and space charge on this method of final focus can be studied. Figure 5 shows the beam envelope for the final focus section.

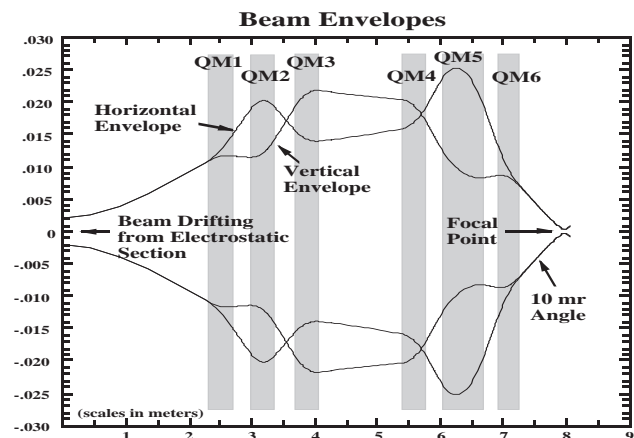


Figure 5: Plot of beam envelopes for magnetic focusing section.

Two-slit scanners measure beam properties after the electrostatic matching section, as well as after the third and sixth magnetic quadrupoles. Measurements of the beam have already been made through the first three magnets with encouraging results, and the second set of three magnets has just been installed, aligned, and pulsed. The beam spot size measurement will be made with a single slit probe that will translate along the beam axis as well as in the transverse directions so as to determine the precise nature of the beam waist.

Subsequently, a separate target injection experiment (section 4.3) may be coupled to the final focus in order to demonstrate the ability to hit a simulated heavy ion fusion target “on the fly”. This will require a set of steering electrodes that have been designed to provide a real time correction to the beam to account for the shot-to-shot variation in target position. The emerging beam from the magnetic section will also be suitable for studying electron neutralization of space charge, and its effect on the focus.

#### 4.3 Fusion Target Injecting and Tracking

An experiment is being conducted at LBNL to investigate and demonstrate the engineering feasibility of accurately injecting and tracking IFE targets into a vacuum chamber [14]. As indicated in figure 6, a gas gun is used to inject non-cryogenic, aluminum and delrin (plastic) target-sized projectiles. These projectiles are optically tracked at three locations using photodiodes to accurately provide real-time transverse and longitudinal target position prediction. This real-time information would then be used to trigger the ion beam and control small beam steering magnets to direct the beam on target.

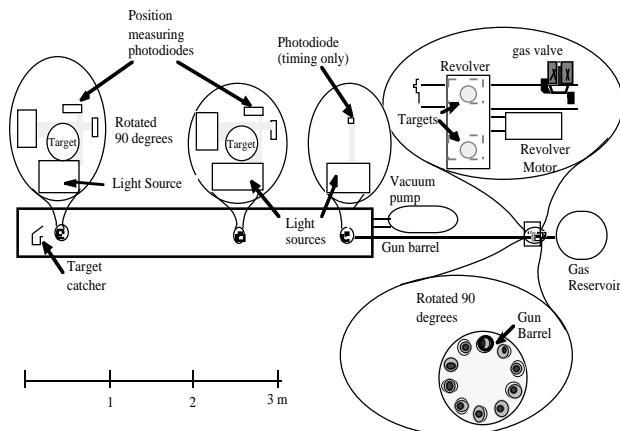


Figure 6: Schematic of Target Injector.

The position prediction is achieved by sending voltage data from one photodiode detector near the gun barrel and another 1 m downstream to a real-time target position prediction circuit. This circuit electronically latches the voltage as the center of the target passes the second detector, and compares this voltage with that when the target is not present. The voltage ratio and the time of passage between these detectors are used to predict the transverse position at which the target passes a third detector located 3 m from the gun barrel. The prediction is in the form of an output voltage that is proportional to the target’s transverse position at detector 3; it is available microseconds after the target passes detector 2.

Although the standard deviation in projectile position in each transverse direction is about 2 mm, a standard deviation of 0.1 mm between predicted and measured positions in both transverse directions is achieved. Using

an up-down counter, the arrival time of the target has been predicted such that the standard deviation in predicted target position along the direction of motion is 0.37 mm. These prediction capabilities are adequate for a heavy ion driver.

## 5 OUTLOOK

The road to a heavy ion IFE power plant is still a long one. Before a machine that achieves fusion with heavy ion beams can be realized, a scaled facility to test many, if not all of the accelerator issues in an integrated way must be built. We plan on being in a position to propose such a facility in a few years. To be in that position, the groups at LBNL and LLNL will continue conducting small experiments to explore issues in HIF.

## 6 ACKNOWLEDGMENTS

I would like to acknowledge the efforts of Joe Kwan, Peter Seidl, David Ponce, Ron Petzoldt, and Steve Maclaren of LBNL and Art Molvik of LLNL for providing the necessary input for this document.

## 7 REFERENCES

- [1] M. Tabak et al., *Nuclear Fusion* **38** (4), 509 (1998).
- [2] R. Moir, “Inertial Fusion Energy Power Plants Based on Laser or Ion Beams,” Proc. of ICENES 98, Tel-Aviv, Israel, June 28 -July 2, 1998, to be published.
- [3] J. W. Kwan et al., “High Current Density Ion Sources for Heavy Ion Fusion Accelerators,” Proc. of Part. Accel. Conf., Vancouver, BC, May 1997.
- [4] A. N. Pargellis and M. Seidl, *J. Appl. Phys.* **49**, 4933 (1978).
- [5] S. Eylon et al., *Il Nuovo Cimento* **106A** (11), 1509 (1993).
- [6] K. K. Chow et al., *Appl. Phys. Lett.* **10**, 256 (1967).
- [7] S.S. Yu et al, *Fusion Engineering and Design* **32-33**, 309, (1996).
- [8] C. M. Celata et al., Proc. of 1987 Part. Acc. Conf., Washington, D.C., **2** 1167 (1987).
- [9] C. M. Celata et al., Proceedings of the 1995 Part. Acc. Conf., 3220 (1995). C. M. Celata et al., *Fusion Eng. and Design*, **32-33**, 219 (1996).
- [10] P. A. Seidl et al., “Progress on the Scaled Beam Combing Experiment at LBNL,” Proc. of Inter. Symp. on Heavy Ion Inertial Fusion, Heidelberg, Germany Sept. 24-27, 1997, to be published in *Nucl. Inst. and Meth. A.*
- [11] L. Ahle et al., “Recent Progress in the Development of a Circular ion Induction Accelerator for Space Charge Dominated Beams at LLNL,” these proceedings.
- [12] A. W. Molvik et al., “Induction Core Performance,” these proceedings.
- [13] A. Tauschwitz et al., *Fusion Eng. and Design*, **32-33**, 493-502 (1996).
- [14] R. Petzoldt, LBNL Report 41360, (1998).